10

Spectroscopy of divalent samarium in caesium iodide single crystals

© D.O. Sofich, R.Yu. Shendrik

Vinogradov Institute of Geochemistry, Siberian Branch, Russian Academy of SciencesIrkutsk, Russia

e-mail: sofich@igc.irk.ru

Received October 28, 2022
Revised December 24, 2022
Accepted March 21, 2023

The article describes the process and parameters of growing $CsI:Sm^{2+}$ single crystals by the Czochralski method. Spectroscopic studies of the $CsI:Sm^{2+}$ single crystal have been carried out; it has been established that samarium ions enter the caesium iodide single crystal in the divalent state. At room temperature, luminescence is observed corresponding to the $4f^5d^1-4f^6$ transitions of divalent samarium; on cooling, only radiative $4f^6-4f^6$ transitions are observed. The temperature dependence of the luminescence has been measured, the barrier energy has been determined, and the decay times of the luminescence have been measured.

Keywords: luminescence, halides, samarium, scintillators, single crystals.

DOI: 10.61011/EOS.2023.05.56508.59-22

Introduction

Divalent samarium ions have recently been considered as an activator for scintillation crystals and phosphors, which is mainly due to their ability to demonstrate $5d-4f$ emission transitions in the red area of the spectrum. The transitions $5d-4f$, unlike the transitions $4f-4f$, are allowed quantum mechanically, therefore they have a shorter decay time and a ́higher oscillator strength [1]. However, unlike $4f$, the $5d$ shell is not shielded from the action of the ligand field, so the properties of the $5d-4f$ transitions strongly depend on the crystal matrix used. In this context, one of the promising directions is the development of scintillators based on halide crystals containing divalent samarium ions, the luminescence of which is in the red area of the spectrum, which makes it promising to use it as a scintillator compatible with avalanche photodiodes [2–7] in luminescent thermometry [8,9], as well as a red phosphor [10].

The ground topic of this paper is the study of the spectral characteristics of a cesium iodide single crystal activated with divalent samarium. We consider cesium iodide as a potentially promising matrix for divalent samarium, where $5d-4f$ emission transitions will be observed.

Cesium iodide — well-known and well-studied crystal – scintillator, has high density and transparency in the visible range [11]. There are papers on the coactivation of $CsI:Tl$ [12,13] crystals by Sm^{2+} ions, where the authors tried to improve the characteristics of the known scintillator. However, the study of the spectral properties of Sm^{2+} ions in CsI crystals is carried out for the first time.

Crystal growing process

CsI(I) crystalline (Lanhit) with a purity of 99.998% (according to metal impurities) and SmI_2 with a purity of 99.99% (Lanhit) were used as initial components. The content of SmI_2 was 1 mol% in the charge. $CsI:Sm^{2+}$ single-crystals were grown from melt by the Czochralski method in a UVK [14] growth unit. The growth unit is an evacuated chamber made of stainless steel with a cooled movable rod. The unit is equipped with a graphite heating unit, the opportunity of inert gas puffing and automated control. The feedstock weighing 150 g was loaded into a preliminarily annealed glassy carbon crucible and dried directly in the growth unit. During the drying process, the feedstock was held for five hours in a vacuum at a temperature of 400°C. At the final stage of drying, the residual vapor pressure in the chamber was less than 0.01 Pa. After drying, high purity argon was injected into the chamber until a pressure of 10 kPa was reached. Seeding was carried out after complete melting of the feedstock on a quartz capillary (Fig. 1). The seed displacement speed was 2.6 mm/h, the seed rotation speed was 3.5 min^{-1}.

At the end of growth, the single-crystal was cooled at a rate of 5 K/min until room temperature was reached. Thus, a transparent colorless single-crystal with a diameter of 12 mm and a length of 80 mm was grown. For spectroscopic studies, crystal samples were prepared in the form of flat polished plates with a thickness of 2 mm.

The resulting single-crystal is not colored. This may indicate a significantly lower concentration of Sm^{2+} in the crystal compared to the initial charge. This is explained by the fact that when the mixture is heated to the melting temperature, SmI_2 hydrolyzes with the formation of samarium oxide. At present, studies are being carried out aimed at reducing the contribution of this process, which will allow to increase the concentration of Sm^{2+} ions in the crystal. Nevertheless, there is intense luminescence in the grown crystal in the red area of the spectrum upon laser excitation at a wavelength of 405 nm (Fig. 2).

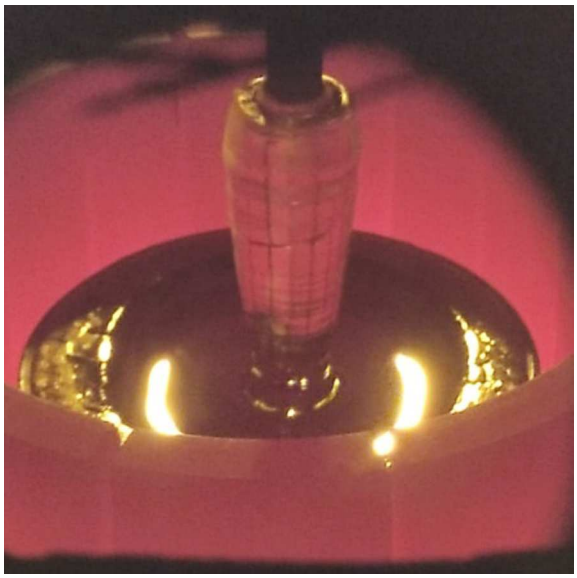

Figure 1. Growing a single-crystal CsI:Sm^{2+} by the Czochralski method.

Research methods

Absorption spectra in the infrared area were recorded using an FT-801 infrared Fourier spectrometer (Simex). The luminescence spectra were measured using an SDL-1 double monochromator with 600 mm^{-1} lattices and a Hamamatsu H10721-04 photomodule. The spectral measurement range of the instrument is 400–800 nm, the value of the inverse linear dispersion is 1.6 nm/mm. The excitation was carried out using a semiconductor laser with a wavelength of 405 nm and a power of 40 mW. The unit is equipped with a vacuum filling cryostat with the opportunity of cooling to the boiling point of liquid nitrogen. Temperature control was carried out using a chromel-alumel thermocouple. The excitation spectrum was obtained using a Perkin-Elmer LS55 luminescent spectrofluorimeter. Luminescence decay curves upon photoexcitation by a pulsed nitrogen laser (wavelength 337 nm, pulse duration 10 ns) were obtained using an MDR-2 monochromator, a Hamamatsu 6780-04 photomodule, and a Rigol DS2202E oscilloscope with a bandwidth of 200 MHz.

Results and discussion

The excitation spectrum (Fig. 3) was measured at room temperature, the recording wavelength was 680 nm. The spectrum consists of a set of bands located in the area 200–650 nm. These bands correspond to the allowed $4f^6$–$4f^5 5d^1$ transitions of divalent samarium. A large number of bands is explained by the mixing of the states $5d^1$ and $4f^5$, while these states are additionally split by the action of the crystal field of the ligands [15–18].

The luminescence spectra of CsI:Sm^{2+} at room temperature and upon cooling to 80 K are shown in Fig. 4.

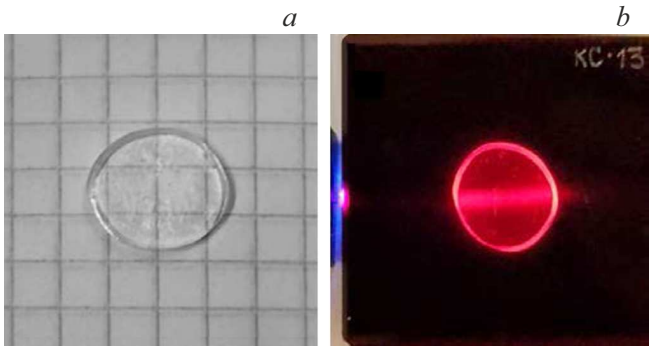

Figure 2. Images of a Cs:Sm^{2+} crystal under daylight (a) and through a KS-13 filter under laser excitation with a wavelength of 405 nm (b).

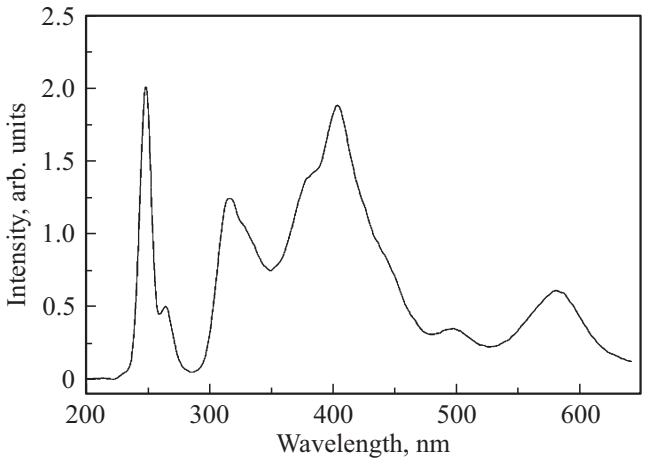

Figure 3. Excitation spectrum of CsI:Sm^{2+} at room temperature. The wavelength of luminescence registration is 680 nm.

The set of bands in the luminescence spectrum at 80 K indicates that samarium ions enter the crystalline matrix in the divalent state. There are $4f^6$–$4f^6$ transitions from the lower excited level $^5D_0$ to the group of levels ^7F_n, where $n = 0, 1, 2$. No bands characteristic of trivalent samarium ions were found [19]. At room temperature, there is a luminescence band in the 600–775 nm area with a maximum at 680 nm and a width at half maximum of 65 nm. This band refers to the $4f^5 5d^1 - 4f^6$ transitions of divalent samarium, while the$4f^6 - 4f^6$ bands disappear completely.

The predominance of the magnetic dipole transition $^5D_0$–$^7F_0$ in the luminescence spectrum at 80 K indicates that the crystalline environment of samarium belongs to the lower symmetry group, which is explained by the presence of a charge compensator near the samarium ion, which distorts the cubic lattice of cesium iodide [20].

The number of Stark bands in the $^5D_0$–$^7F_1$ and $^5D_0$–$^7F_2$ transitions is 3 and 5, respectively. Summarizing the above, we can conclude that the crystalline environment of divalent samarium ions has one first-order rotational symmetry axis (C_1) or one symmetry plane (C_s) [21].

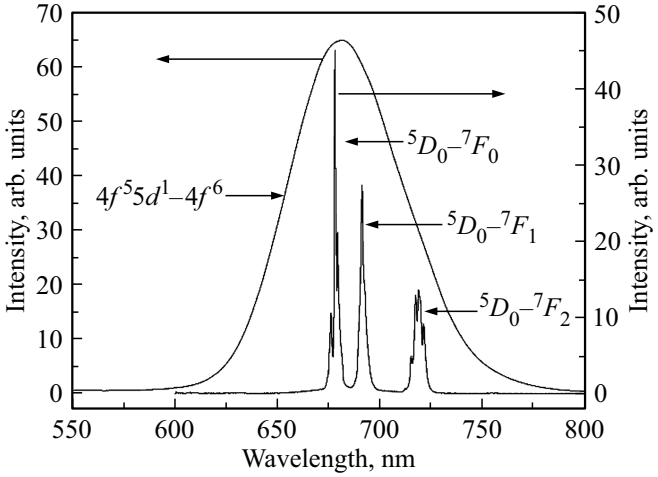

Figure 4. Luminescence spectra of CsI : Sm^{2+} at room temperature (left y-axis) and at 80 K (right y-axis). Laser excitation at a wavelength of 405 nm was used.

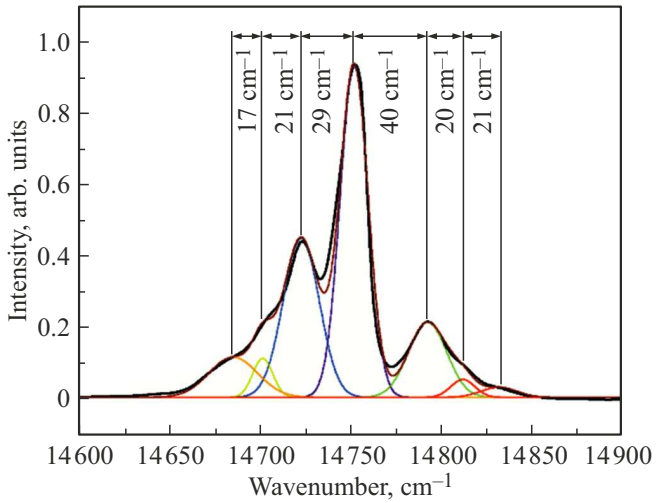

Figure 5. Approximation by Gaussian functions of a section of the spectrum in the transition area $^5D_0 - ^7F_0$.

However, the large number of bands in the $^5D_0 - ^7F_0$ transition, which has one degenerate state, should be explained. The Gaussian approximation of the transition band $^5D_0 - ^7F_0$ is presented in Fig. 5. The vertical lines correspond to the maximum of each band, the arrows indicate the difference in energy between adjacent bands. The splitting of this band is typical for complex compounds, where several divalent samarium luminescence centers with different symmetry are possible, however, in our case, the $^5D_0 - ^7F_1$ and $^5D_0 - ^7F_2$ transitions have a rather ordered structure. In addition, it is difficult to assume the existence of seven different configurations of samarium centers in a CsI crystal (as can be seen from the figure, the transition is described by seven Gaussian functions).

Raman shifts for cesium iodide are known from the literature [22] and are in good agreement with the energy

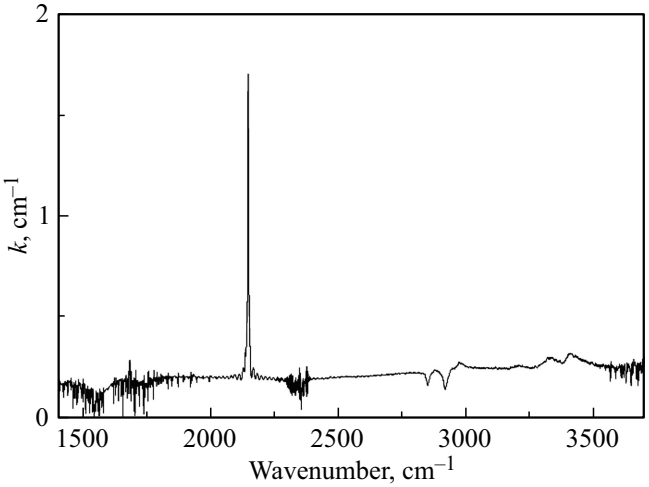

Figure 6. Absorption spectrum of a CsI : Sm^{2+} crystal in the infrared area.

Temperature dependence approximation parameters

Band of luminescence	Energy barrier, cm^{-1}	Coefficient determination R^2
$4f^6 - 4f^6$	840 ± 6	0.9934
$4f^5 5d^1 - 4f^6$	785 ± 5	0.9925

differences between the peaks shown in the figure. Based on the above stated, we explain the splitting of the $^5D_0 - ^7F_0$ spectral band by the presence of an electron-vibrational interaction with the crystal lattice of cesium iodide.

Divalent samarium ions in a CsI crystal replace monovalent cesium ions, in this case a cation vacancy, an interstitial iodine ion, or an impurity oxygen [23] can serve as a charge compensator. However, oxygen centers in CsI crystals have not been found earlier. In the crystals grown in air, intense absorption was observed in the infrared region of the spectrum, associated with OH- [24] hydroxyl anions. In the absorption spectrum in the infrared area (Fig. 6) there is a band with a maximum in the area of 2143 cm^{-1} , which is associated with stretching vibrations C−O in the CO molecule. This may indicate reducing conditions during crystal growth [25]. Absorption associated with hydroxyl ions was not found. Small absorption bands in the area of 3400 cm^{-1} are associated with adsorbed water on the crystal surface.

To determine the energy barrier between the levels of the $4f$ and $5d$ shells of the samarium ion shells, we measured the temperature dependences of the luminescence intensity of $4f^6 - 4f^6$ and $4f^5 5d^1 - 4f^6$ (Fig. 7). The figure shows an anticorrelation between the temperature dependences.

In order to estimate the value of the interval between two interacting excited states $4f^6(^5D_0)$ and $4f^5 5d^1$, the temperature dependences were approximated using the Mott function [26]. The resulting values are summarized in the table.

The relatively low energy of the barrier between the excited levels $4f$ and $5d$ of divalent samarium explains the quenching of the $4f^5 5d^1 - 4f^6$ luminescence upon cooling of the crystal. On the other hand, at temperatures over 130 K, the phonon-stimulated process of electron transfer to the excited levels of the $5d$ shell of samarium ions begins to predominate.

Fig. 8 shows the measured luminescence decay curves, the intensity is given on a logarithmic scale, and the excitation was performed by a pulsed nitrogen laser. The luminescence decay time was measured at the maximum of the $4f^5 5d^1 - 4f^6$ (680 nm) and $4f^6 - 4f^6$ (678 nm) emission bands at 293 K and 80 K, respectively. Approximation

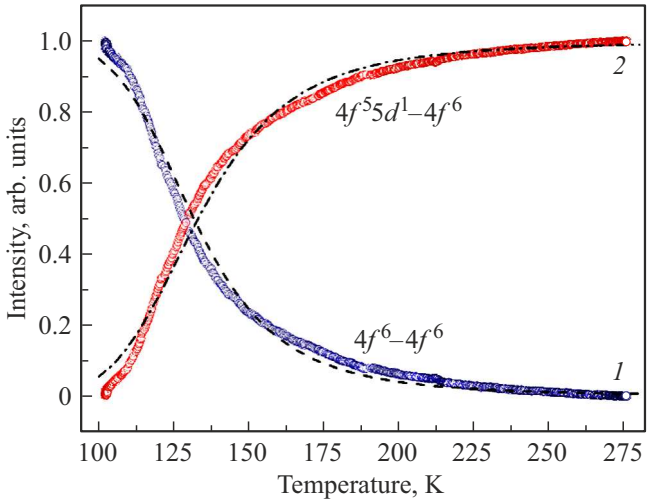

Figure 7. Temperature dependences of the luminescence intensity in the $4f^6 - 4f^6$ (*1*) and $4f^5 5d^1 - 4f^6$ (*2*) transitions of Sm^{2+} ions. The intensities are normalized to unity. Dashed and dash-dotted lines — approximations by the Mott function.

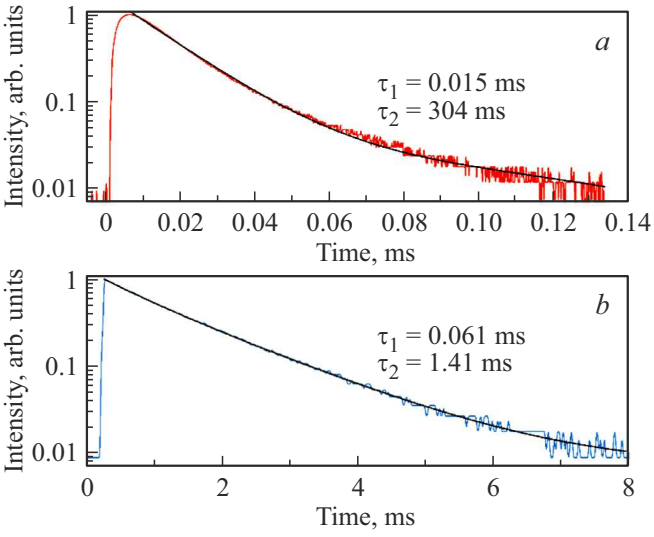

Figure 8. Oscillograms of the luminescence decay of the $4f^5 5d^1 - 4f^6$ (680 nm) band at room temperature (*a*) and the $^5D_0 - ^7F_0$ (678 nm) band at 80 K (*b*).

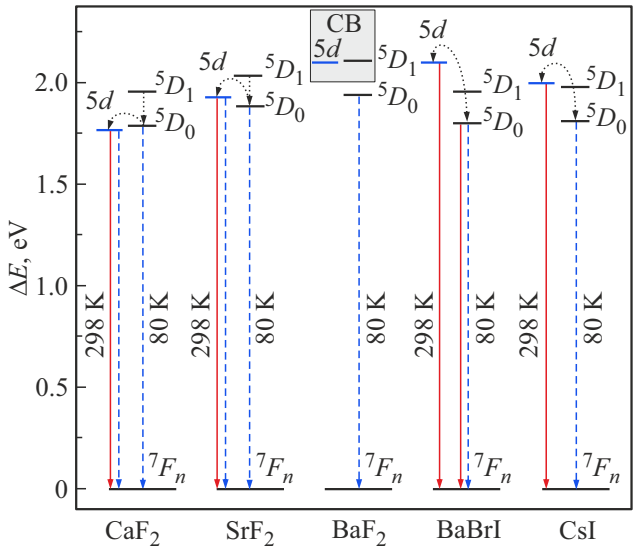

Figure 9. Diagram of energy transitions of Sm^{2+} ions in a series of halogen compounds. The vertical arrows show the observed emission transitions at 298 K and 80 K (dotted line).

of curves showed that in both cases the luminescence decay kinetics can be approximated by the sum of two exponential functions. At room temperature, the fast component has a decay time of 15 μs, and the slow one — 304 ms.

When cooled to 80 K, the $^5D_0 - ^7F_0$ band also contains a long component with a duration of 1.41 ms characteristic of $4f^6 - 4f^6$ transitions, as well as fast luminescence with a decay time of 61 μs.

We explain the observation of several damping components by the presence of mixed states $4f$ and $5d$, in which competing processes occur upon photoexcitation of divalent samarium ions.

On the basis of the resulting data, as well as data from the papers [27,28], a diagram of energy transitions was constructed for a number of halogen crystals containing divalent samarium (Fig. 9). The diagram shows the mutual arrangement of the $4f$ and $5d$ states of samarium ions, as well as the observed emission transitions. The ground state $^7F_0$ was taken as zero.

Conclusions

A single-crystal of cesium iodide with an admixture of divalent samarium was grown and studied by spectroscopic methods. The excitation and luminescence spectra were measured and interpreted, the temperature dependence and energy of the barrier between the $4f$ and $5d$ shells of samarium ions were determined, and the luminescence decay time at various temperatures was measured.

It is shown that samarium ions enter the crystal in the divalent state and have a low-symmetry ligand field due to the presence of a charge compensator. The resulting crystal exhibited intense luminescence of $4f^5 5d^1 - 4f^6$ at

room temperature and luminescence of $4f^6-4f^6$ at a temperature of 80 K, measurements of the temperature dependence showed an anticorrelation between the luminescence intensity of these transitions. The energy of the barrier between the levels $4f$ and $5d$ of the shells of the samarium ion was determined.

The $CsI:Sm^{2+}$ crystal proved to be promising from the point of view of luminescent thermometry due to the low energy of the barrier between the $4f$ and $5d$ shells of samarium ions. In further studies, it will be required to focus on increasing the concentration of samarium ions in a crystal, which involves studying the nature of the charge compensator for bivalent samarium and varying the growth conditions of single-crystals. If we consider this crystal as a scintillator, then it will be required to conduct studies aimed at reducing the decay time of the luminescence of $4f^55d^1-4f^6$ samarium ions.

Funding

Growing and spectroscopic studies of crystals were carried out as part of the state assignment № 0350-2016-0024 „Crystalline and amorphous functional materials with predictable properties".

Conflict of interest

The authors declare that they have no conflict of interest.

References

[1] M. Suta, C. Wickleder. J. Luminescence, **210**, 210 (2019). DOI: 10.1016/j.jlumin.2019.02.031.
[2] P. Dorenbos. Optical Materials: X, **1**, 100021 (2019). DOI: 10.1016/j.omx.2019.100021
[3] A.A. Shalaev, R.Y. Shendrik, A.I. Rusakov, Y.V. Sokol'nikova, A.S. Myasnikova. Physic. Solid State, **61** (12), 2403 (2019). DOI: 10.1134/S1063783419120497.
[4] D. Sofich, R. Shendrik, A. Rusakov, A. Shalaev, A. Myasnikova. AIP Conference Proceedings, **2392**, 040004 (2021). DOI: 10.1063/5.0061794
[5] A. Shalaev, R. Shendrik, A. Rusakov, A. Bogdanov, V. Pankratov, K. Chernenko, A. Myasnikova. Nuclear Instruments and Methods in Physics Research Section B: Beam Interactions with Materials and Atoms, **467**, 17 (2020). DOI: 10.1016/j.nimb.2020.01.023
[6] W. Wolszczak, K.W. Krämer, P. Dorenbos. J. Luminescence, **222**, 117101 (2020). DOI: 10.1016/j.jlumin.2020.117101
[7] A. Tuomela, M. Zhang, M. Huttula, S. Sakirzanovas, A. Kareiva, A.I. Popov, A.P. Kozlova, S. Assa Aravindh, W. Cao, V. Pankratov. J. Alloys and Compounds, **826**, 154205 (2020). DOI: 10.1016/j.jallcom.2020.154205
[8] M. Runowski, P. Woźny, V. Lavin, S. Lis. Sensors and Actuators B: Chemical, **273**, 585 (2018). DOI: 10.1016/j.snb.2018.06.089
[9] Z. Cao, X. Wei, L. Zhao, Y. Chen, M. Yin. ACS Applied Materials & Interfaces, **8** (50), 34546 (2016). DOI: 10.1021/acsami.6b10917
[10] T.H. Quang Minh, N. H. Khanh Nhan, N.D. Quoc Anh, H.Y. Lee. J. Chinese Institute of Engineers, **40** (4), 313 (2017). DOI: 10.1080/02533839.2017.1318720
[11] W. Cheng, P.S. Liu, M.J. Ying, F.S. Zhang. Nuclear Science and Techniques, **33** (3), 1 (2022). DOI: 10.1007/s41365-022-01020-2
[12] V.V. Nagarkar, S.C. Thacker, V. Gaysinskiy, L.E. Ovechkina, S.R. Miller, S. Cool, C. Brecher. IEEE transactions on nuclear science, **56** (3), 565 (2009). DOI: 10.1109/TNS.2009.2016198
[13] R.H. Bartram, L.A. Kappers, D.S. Hamilton, A. Lempicki, C. Brecher, V. Gaysinskiy, V.V. Nagarkar. IEEE Transactions on Nuclear Science, **55** (3), 1232 (2008). DOI: 10.1109/TNS.2008.922833
[14] A. Rupasov, A. Shalaev, R. Shendrik. Crystal Growth & Design, **20** (4), 2547 (2020). DOI: 10.1021/acs.cgd.9b01678.
[15] M. Guzzi, G. Baldini. J. Luminescence, **6** (4), 270 (1973). DOI: 10.1016/0022-2313(73)90023-9
[16] M.N. Sundberg, H.V. Lauer, F.K. Fong. J. Chem. Phys., **62** (5), 1853 (1975). DOI: 10.1063/1.430669
[17] M. Karbowiak, P. Solarz, R. Lisiecki, W. Ryba-Romanowski. J. Luminescence, **195**, 159 (2018). DOI: 10.1016/j.jlumin.2017.11.012
[18] A. Meijerink, G.J. Dirksen. J. Luminescence, **63** (4), 189 (1995). DOI: 10.1016/0022-2313(94)00064-J
[19] S.L. Walker, C.H. Drozdowski, J. Gharavi-Naeini, N.A. Stump. Appl. Spectrosc., **73** (5), 550 (2019). DOI: 10.1177/0003702818815180
[20] C.H. Drozdowski, J. Gharavi-Naeini, N.A. Stump. Appl. Spectrosc., **71** (7), 1684 (2017). DOI: 10.1177/0003702817694900
[21] P.A. Tanner. Chemical Society Reviews, **42** (12), 5090 (2013). DOI: 10.1039/C3CS60033E
[22] H.H. Lal, V.P. Verma. J. Physics C: Solid State Physics, **5** (10), 1038 (1972). DOI: 10.1088/0022-3719/5/10/008
[23] H. Vrielinck, D.G. Zverev, P. Leblans, J.P. Tahon, P. Matthys, F. Callens. Phys. Rev. B, **85** (14), 144119 (2012). DOI: 10.1103/PhysRevB.85.144119
[24] A. Gektin, N. Shiran, S. Vasyukov, A. Belsky, D. Sofronov. Opt. Mater., **35** (12), 2613 (2013). DOI: 10.1016/j.optmat.2013.07.029
[25] L.P. Smol'skaya, V.V. Dorokhova. J. Applied Spectroscopy, **52** (1), 29 (1990). DOI: 10.1007/BF00664775
[26] N. Mott, R. Gurney. UFN, **44** (3), 482 (1951). (in Russian).
[27] E. A. Radzhabov. Opt. Mater., **85**, 127 (2018). DOI: 10.1016/j.optmat.2018.08.044
[28] A.A. Shalaev, R. Shendrik, A.S. Myasnikova, A. Bogdanov, A. Rusakov, A. Vasilkovskyi. Opt. Mater., **79**, 84 (2018). DOI: 10.1016/j.optmat.2018.03.017

Translated by E.Potapova